JOURNAL OF CHEMICAL & ENGINEERING DATA

ARTICLE

pubs.acs.org/jced

Osmolality and Unfrozen Water Content of Aqueous Solution of Dimethyl Sulfoxide

Lindong Weng, Weizhong Li,* Jianguo Zuo, and Cong Chen

Key Laboratory of Ocean Energy Utilization and Energy Conservation of Ministry of Education, Dalian University of Technology, Dalian, Liaoning Province, P.R. China 116024

ABSTRACT: Dimethyl sulfoxide is one of the most popular cryoprotectants in cryobiology. It is crucial for the successful cryopreservation to quantitatively analyze the cryoprotective properties of dimethyl sulfoxide. In this study, the osmolality and the unfrozen water content of the aqueous solution of dimethyl sulfoxide are determined using a Perkin-Elmer Diamond DSC. For precisely calculating the unfrozen water content, this study takes into consideration the effect of dilution on the enthalpy of fusion in the solution which is a commonly neglected factor. The osmotic virial representation and the quantitative relationships between the unfrozen water content and the solution composition are reported. The experimental results show that the aqueous dimethyl sulfoxide solution has a greatly depressed freezing point and a large osmolality. Moreover, the water-blocking ability of dimethyl sulfoxide weakens when the solution is more concentrated. The results in this study will enlarge the database of physical and chemical properties of dimethyl sulfoxide and reinforce our understanding of the cryoprotective mechanisms of dimethyl sulfoxide in aqueous solutions.

INTRODUCTION

Dimethyl sulfoxide (DMSO) enjoys a wide range of applicability as a solvent in chemical and biological processes involving both plants and animals.[1] Therefore, the unique physical and chemical properties of DMSO have been extensively studied so far.[2−9] It was found that thermodynamic properties of the aqueous DMSO solution exhibit strong deviations from ideality.[2] DMSO molecules can perturb the "water structure" by forming strong hydrogen bonds with water molecules[4] and enhance the remaining water−water hydrogen-bonding network.[3]

Owing to its unparalleled properties DMSO has been the preferred cryoprotective agent (CPA) in the applications of cryopreservation. Plenty of studies of the cryoprotective properties of DMSO have been initiated since the discovery of its cryobiological advantage by Lovelock and Bishop[10] in 1959. The solid−liquid phase diagrams of DMSO/water and DMSO/sodium chloride/water mixtures were determined through thermal analysis techniques.[11−13] Hey and MacFarlane[14,15] investigated the crystallization behaviors of ice in the DMSO solution. Since vitrification has been proved to be a promising method of cryopreservation, the glass-forming tendency and stability of the aqueous DMSO solution were also evaluated.[16]

The cryoprotective properties of DMSO can help enhance the post-thaw viability of cells and tissues in cryopreservation.[17,18] However, little is known about the underlying cryoprotective mechanisms of CPAs like DMSO.[17] Specifically, the quantitative understanding of the ability of DMSO to intensify the water transport across cell membranes and its ability to inhibit the intracellular ice formation is still insufficient. There have been some studies of the osmolality of the DMSO/water mixture based on the osmotic virial equations,[19−22] but further investigations are still necessary. On the other hand, the conventional calculation of the unfrozen water content based on the "lever rule" is subject to the assumption that ice is in equilibrium with the residual solution. Little attention has been paid to the determination of the unfrozen water content in the aqueous solution of DMSO under nonequilibrium freezing conditions. DSC measurement is a widely used approach to determine the unfrozen water content in polymer solutions under nonequilibrium freezing conditions,[23−25] but it has rarely been employed in cryobiology. In addition, the effect of dilution on the enthalpy of fusion in the solution was neglected in previous studies for simplifying the calculation of the unfrozen water content.[23−26] However, such a simplification can cause the significant loss of the calculation accuracy when the change brought forth by the dilution heat is noticeable.

In the present study, DSC determinations of the osmolality and the unfrozen water content of the aqueous DMSO solution with compositions of cryobiological interest are undertaken. The dissolution of DMSO in water can generate a non-negligible amount of heat. Therefore, the effect of dilution caused by the melting of ice in the solution is considered for calculating the unfrozen water content precisely. As a result, the osmotic virial equation of the aqueous DMSO solution and the quantitative relationships between the unfrozen water content and the molality of the solution are obtained.

METHODOLOGY

Materials. DMSO with the initial mass-fraction purity of 99.5 % is used in our experiment. It is purchased from Kermel Chemical Reagent Co. Ltd. (Tianjin, P.R.China) without further purification. DMSO as the solute and the reverse osmosis and deionized (RO/DI) water as the solvent are mixed into solutions

Received: March 15, 2011
Accepted: June 8, 2011
Published: June 21, 2011

dx.doi.org/10.1021/je2002607 | *J. Chem. Eng. Data* 2011, 56, 3175–3182

of (1, 2, 3, 5, 7, and 9) mol·kg^{-1}. The RO/DI water is produced by the Hitech-Kflow laboratory water purification system (Hogon Scientific Instrument Co. Ltd., Shanghai, P.R.China). Three samples of each molality are prepared for repetitive measurements. Each sample (3−4 mg) is sealed in an aluminum sample pan by the volatile sample sealer kit (Perkin-Elmer Corp., Norwalk, CT, U.S.A.).

DSC Measurement. A Diamond DSC (Perkin-Elmer Corp., Norwalk, CT, U.S.A.) is employed in our experiment. It is equipped with a TAGS gas station and an intracooler 2P cooling accessory (i.e., a mechanical refrigerator) which can provide a stable cryogenic environment as low as −85 °C. The thermogram of each sample subjected to the cooling and subsequent warming protocols can be recorded and the phase transitional behavior of the sample can be also real-time tracked by the DSC equipment.

A two-point temperature calibration is conducted using *n*-decane (melting temperature: −29.66 °C) and RO/DI water (melting temperature: 0 °C) as standard samples, prior to our experiment. The *n*-decane (mass-fraction purity >99.5%) is purchased from Sinopharm Chemical Reagent Co. Ltd. (Shanghai, P.R.China) without further purification. The scheme of the temperature calibration is as follows: the temperature range is from (−60 to +30) °C and the scanning rate is 5 °C·min^{-1}. The heat flow scale is calibrated against the enthalpy of fusion in pure water (333.5 J·g^{-1}) during the warming protocol with a rate of 5 °C·min^{-1}.

In our DSC measurement, each sample is cooled to −50 °C and then held at this temperature for 5 min so that the freezable water in the sample can be completely crystallized, leaving the solute and the unfrozen water in the remaining liquid phase. Afterward, the sample is heated to 25 °C at a rate of 5 °C·min^{-1}. The warming thermogram containing the melting endotherm is recorded by the Pyris software installed in a Dell Precision T3400 workstation (Dell Inc., Round Rock, Texas, U.S.A.). Finally, the endothermic peak area A and the peak temperature t_P are determined based on the warming thermogram with the sigmoidal baseline. The peak temperature t_P is determined to be the melting temperature t_m of the sample as previously shown.[27] The thermal lag is negligible in our experiment due to the slow scanning rate (5 °C·min^{-1}) and the small sample size [(3−4) mg]. Hence, no further temperature corrections are needed.

Calculation of the Osmolality. The osmolality π in Osm can be calculated according to the melting temperature t_m in °C by the following equation:[22]

$$\pi = \frac{t_m^0 - t_m}{[M_w/(s_w^{0\,L} - s_w^{0\,S})]R(t_m + 273.15)} \quad (1)$$

where t_m^0 is the melting temperature of ice in pure water (0 °C), M_w the molar mass of water (0.01802 kg·mol^{-1}), s_w^{0L} and s_w^{0S} the molar entropies of pure liquid water and pure ice, respectively. The difference between s_w^{0L} and s_w^{0S} is 22.00 J·mol^{-1}·K^{-1}. R is the universal gas constant (8.314 J·mol^{-1}·K^{-1}).

A truncated second-order osmotic virial equation for the single-solute system is used in this study to obtain the second osmotic virial coefficient.[19]

$$\pi = m + B \cdot m^2 \quad (2)$$

where m is the molality of the solution in mol·kg^{-1} and B the second osmotic virial coefficient in (mol·kg^{-1})$^{-1}$.

The osmolality can be correlated with the molality of the solution according to the following equation as well.[28]

$$\pi = \varphi \upsilon m \quad (3)$$

where υ is the dissociation coefficient of the solute. Specifically, $\upsilon = 1$ for DMSO[29] and φ is the osmotic coefficient which varies with the solution composition.

Thereby, π of the aqueous DMSO solution can be quantified according to our experimental data on the melting temperature t_m. Meanwhile, it can be evaluated in terms of either B or φ.

Calculation of the Unfrozen Water Content. In this study, the unfrozen water (or the bound water) is defined as the water that has not been transferred into its solid phase at −50 °C. The water that has solidified at −50 °C is considered as the freezable water (or the free water). The amount of the unfrozen water can be calculated by subtracting the freezable water content from the total amount of water in the solution. For determining the amount of the freezable water, the effective enthalpy of fusion L_e is introduced which is the algebraic addition of the enthalpy of fusion in the solution and the heat generated by the dissolution of DMSO in the melted ice.

The detailed procedures of calculating the unfrozen water content are explained as follows:

The freezable water content W_f, in mg, can be calculated with the following equation.

$$W_f = \frac{A}{L_e} \quad (4)$$

where A, in mJ, is the peak area covered by the melting endothermic peak above the scanning baseline in the DSC thermogram. L_e can be expressed as follows:[30,31]

$$L_e = L_0 - \Delta H - Q_d \quad (5)$$

where L_0 is the enthalpy of fusion in pure water (333.5 J·g^{-1}), ΔH, in J·g^{-1}, is the decrement of the enthalpy difference between water and ice caused by the freezing point depression and Q_d, in J·g^{-1}, is the heat generated when ice melts into the solution.

ΔH can be obtained according to the following equation as reviewed previously:[30]

$$\Delta H = \int_{t_m}^{0} (c_w - c_i)\, dt \quad (6)$$

where c_w and c_i are the specific heat capacities of water and ice, respectively, in J·g^{-1}·°C^{-1}.

Angell et al.[32] measured the specific heat capacity of water at the extreme of the supercooling. The specific heat capacity of ice in a temperature range of (0 to ∼−258) °C was reported by Giauque and Stout.[33] In our study, the values of c_w covering the temperature range of (0 to ∼−40) °C and those of c_i covering the temperature range of (0 to ∼−100) °C are calculated with the following representations. These two equations are obtained by fitting the above-mentioned experimental data to them, respectively.

$$c_w = 4.287 + 0.031t + 0.004t^2 + 1.890 \times 10^{-4}t^3 + 3.261 \times 10^{-6}t^4 \quad (7)$$

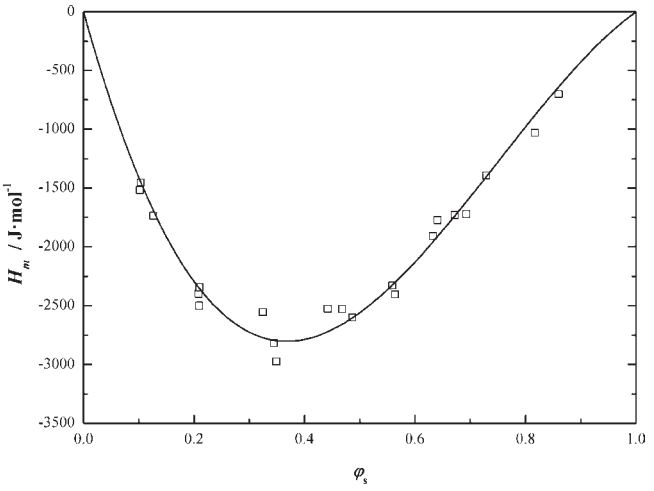

Figure 1. H_m of aqueous DMSO solutions of φ_s ranging from 0 to 1 at 25 °C; H_m, heat of mixing; φ_s, mole fraction of DMSO in the solution; —, results of H_m at 25 °C calculated with eq 10; □, experimental data reported by Clever and Pigott.[38]

The goodness of fit R^2 is 0.9991.

$$c_i = 2.109 + 0.008t + 2.592 \times 10^{-6}t^2 \quad (8)$$

The goodness of fit R^2 is 0.9998.

Based on the theory proposed by Kumano et al.,[31] the dilution heat Q_d can be calculated according to the following equation. In this study, the equation has been slightly modified for illustrative clarity.

$$Q_d = \frac{x_s^2}{100} h_m' \quad (9)$$

where h_m is the heat of mixing in J·g^{-1} and x_s the mass fraction of the solute in the solution.

h_m, in J·g^{-1}, refers to the heat in J generated when 1 g solute is solvated into enough water to produce the solution of a given mass fraction x_s. H_m, in J·mol^{-1}, represents the heat in J generated by making 1 mol solution of a given mole fraction φ_s. Given that the relationship $H_m \sim \varphi_s$ can be converted into the relationship $h_m \sim x_s$, the effective enthalpy of fusion L_e can be obtained if the relationship $H_m \sim \varphi_s$ is known.

The Redlich−Kister (RK) equation[34] is commonly employed to represent the thermodynamic properties such as heat of mixing H_m of the nonideal solution.[35,36] The interaction parameters in the RK equation are subject to the temperature. Kaptay[37] developed a representation to evaluate the effect of temperature on the interaction parameters in the RK equation. The following equation proposed by Kaptay[37] is used in this study for evaluating the composition and temperature dependences of H_m.

$$H_m = \varphi_s(1-\varphi_s)\sum_{i=0}^{n} h_{0i}\left(1+\frac{t+273.15}{\tau_{0i}}\right) exp\left(-\frac{t+273.15}{\tau_{0i}}\right)(2\varphi_s-1)^i \quad (10)$$

where h_{0i} and τ_{0i} are the interaction parameters. In this study, the maximum power n in eq 10 is set to 1 and the experimental data[38] on H_m of the aqueous DMSO solution at 25 °C is fit to eq 10 to obtain the values of the interaction parameters. Finally, the values of the interaction parameters in eq 10 are: $h_{00} = -10239.6$ J·mol^{-1}, $\tau_{00} = 66408.7$ K, $h_{01} = 6847.8$ J·mol^{-1}, and $\tau_{01} = 12570.8$ K. The results of H_m of the aqueous DMSO solution at 25 °C calculated with eq 10 and the experimental data[38] are graphically displayed in Figure 1. The goodness of fit R^2 is 0.9679.

t_m of the aqueous DMSO solution can be solely correlated with φ_s, as explained later. Hence, eq 10 can describe the relationship $H_m \sim \varphi_s$ when t in eq 10 is kept to be t_m. Hitherto, the mass of the freezable water W_f can be obtained according to eqs 4−10.

The mass of the total water W_t in mg and that of the solute W_s in mg in the solution can be expressed as the following equations:

$$W_t = W\frac{1}{1+mM_s} \quad (11)$$

$$W_s = W\frac{mM_s}{1+mM_s} \quad (12)$$

where W is the total mass of the solution in mg and M_s the molar mass of DMSO (0.07813 kg·mol^{-1}).

The mass of the unfrozen water W_{uf} can be obtained by

$$W_{uf} = W_t - W_f \quad (13)$$

The amount of the unfrozen water in mmol is $N_{uf} = W_{uf}/(1000 \cdot M_w)$ and the amount of the solute in mmol is $N_s = W_s/(1000 \cdot M_s)$.

In our study, two criteria are employed to quantitatively evaluate the unfrozen water content in the solution. They are W_{uf}/W_t and N_{uf}/N_s. In detail, W_{uf}/W_t refers to the mass fraction of the unfrozen water out of the total water in the solution and N_{uf}/N_s indicates the ability of DMSO to block water in their mixtures.

Conventionally, the "lever rule" can be used to determine the unfrozen water content if one assumes that ice is in equilibrium with the residual solution. Such an assumption can hold only in equilibrium freezing conditions. The equation takes the form $W_{uf}/W_t = m/m(t)$, where $m(t)$ is the molality of the solution in equilibrium with ice at the desired subzero temperature t (−50 °C in this study). One can calculate $m(t)$ from the liquidus curve. Further, $N_{uf}/N_s = 1/(m(t)M_w)$.

However, when cooling is not infinitely slow and the solution becomes more concentrated as ice crystallization proceeds, an increasing supercooling and a large increase in the viscosity of the unfrozen phase occur. Consequently, freezing becomes progressively slower since ice crystallization is hindered and consequently more time is required for lattice growth at every temperature. Therefore, the above-mentioned assumption cannot hold under such nonequilibrium freezing conditions, where eqs 4−13 will be sufficient to produce the accurate determination of the unfrozen water content.

RESULTS AND DISCUSSION

Melting Temperature of the Aqueous DMSO Solution. The numerical data on the melting temperature of the aqueous solution of DMSO are listed in Table 1. The quantitative relationship between the melting temperature and the solution composition is commonly represented by a polynomial equation.[39−41] Therefore, the melting temperature t_m of the aqueous DMSO solution is correlated with its molality m through a quartic polynomial like eq 14 in this study.

$$t_m = a_1 m + b_1 m^2 + c_1 m^3 + d_1 m^4 \quad (14)$$

dx.doi.org/10.1021/je2002607 |J. Chem. Eng. Data 2011, 56, 3175–3182

Table 1. Melting Temperature t_m of DMSO/Water Binary Mixtures of Molalities m of Cryobiological Interest and the Corresponding Standard Deviation σ

m	t_m	σ
mol·kg^{-1}	°C	°C
1	−1.62	0.15
2	−4.21	0.19
3	−6.95	0.11
5	−13.03	0.16
7	−19.73	0.05
9	−27.48	0.01

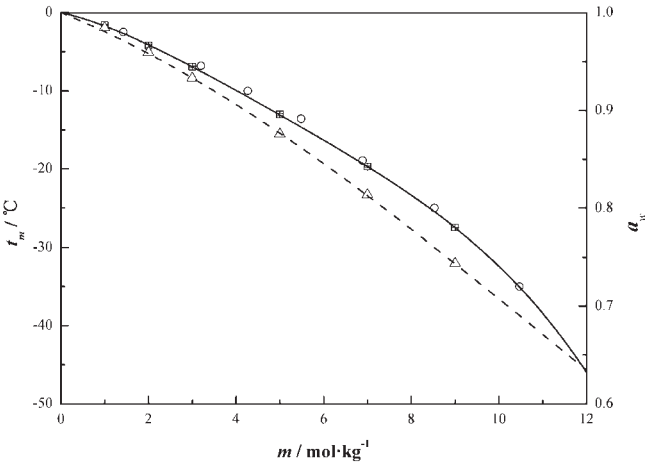

Figure 2. t_m and a_w of aqueous DMSO solutions with compositions of cryobiological interest; t_m, the melting temperature; a_w, the activity of water; m, molality; —, results of t_m calculated with eq 14; — — —, results of a_w calculated by the relation $\pi \sim a_w$ and eq 2; □, experimental data of t_m determined in our DSC experiment; ○, experimental data of t_m reported by Rasmussen and MacKenzie;[11] Δ, a_w determined in our DSC experiment.

where a_1, b_1, c_1, and d_1 are the polynomial coefficients, equal to −1.29517 °C·(mol·kg^{-1})$^{-1}$, −0.49579 °C·(mol·kg^{-1})$^{-2}$, 0.06241 °C·(mol·kg^{-1})$^{-3}$, and −0.00323 °C·(mol·kg^{-1})$^{-4}$, respectively. The goodness of fit R^2 is 0.9982. Figure 2 displays the results of t_m determined in our experiment and those reported in the previous study.[11] The best-fitting curve calculated according to eq 14 is presented in this figure as well. It is clear that the results determined in our experiment have a good quantitative agreement with those reported previously.

It is demonstrated that DMSO depresses the freezing point of its aqueous solution more greatly than some of the alcohols such as ethylene glycol (EG) and glycerol, corresponding to a given concentration. In detail, t_m of EG/water and glycerol/water mixtures of 5 mol·kg^{-1} is −10.53 and −11.28 °C, respectively.[41] The 5 mol·kg^{-1} aqueous DMSO solution has an average melting point of −13.03 °C, at least 1.75 °C lower, as measured in our experiment. Most importantly, it is found that such an advantage of DMSO to depress the freezing point can be more pronounced as the solution becomes more concentrated. Similar findings were also reported previously.[14] For instance, the aqueous DMSO solution of x_s = 45 % depressed the melting temperature of ice in the solution approximately by 34 °C (namely, t_m = −34 °C) while the glycerol solution of the same mass fraction has a t_m = −20.5 °C.[14]

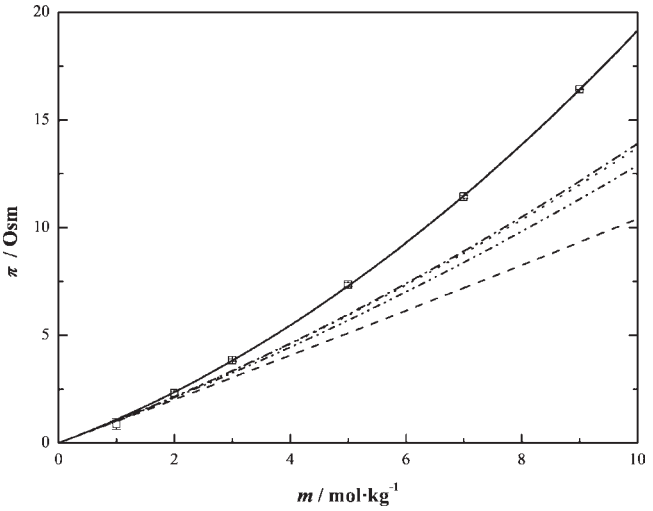

Figure 3. π of CPA/water binary mixtures with compositions of cryobiological interest; π, osmolality; m, molality; —, curve for DMSO/water; — — —, curve for methanol/water; ···, curve for EG/water; —·—, curve for PG/water; —··—, curve for glycerol/water; □, results of DMSO calculated based on our experimental data. Curves are calculated with eq 2.

Table 2. Second Osmotic Virial Coefficient B for Five Commonly-Employed CPAs (i.e., DMSO, Methanol, EG, PG, and Glycerol)

CPA	DMSO	methanol	EG	PG	glycerol
B/(mol·kg^{-1})$^{-1}$	0.092	0.004[a]	0.037[a]	0.039[a]	0.023[a]

[a] Reference 22.

From the cryobiological viewpoint, DMSO in the cytoplasm can more effectively alleviate the supercooling of the intracellular media, compared with other alcohol CPAs. Consequently, the occurrence of the ice crystallization in cells subjected to the freezing protocol can be postponed more greatly when DMSO exists intracellularly. This phenomenon can in part be attributed to strong interactions between DMSO and water molecules.[13] In other words, DMSO molecules can inhibit water molecules from attending the intracellular ice crystallization through DMSO—water hydrogen bonds.[3,4]

Osmolality of the Aqueous DMSO Solution. The relationship $\pi \sim m$ of the aqueous DMSO solution described by eq 2 is shown in Figure 3. The relationships $\pi \sim m$ of the aqueous solutions of other four commonly used CPAs involving methanol, EG, propylene glycol (PG) and glycerol are also presented according to their osmotic virial coefficients published previously[22] (as listed in Table 2). The osmotic coefficient φ for DMSO and the above-mentioned four alcohol CPAs calculated with eq 3 are presented in Figure 4. Moreover, given that $\ln(a_w) = -\pi M_w$, one can calculate the activity of water a_w in the aqueous DMSO solution at t_m. The results of a_w have been presented in Figure 2.

The second osmotic virial coefficient B for DMSO is determined to be 0.092 in this study. The goodness of fit R^2 of eq 2 is 0.9809. The values reported previously are 0.0843[21] and 0.108,[22] respectively. These differences may be attributed to the different

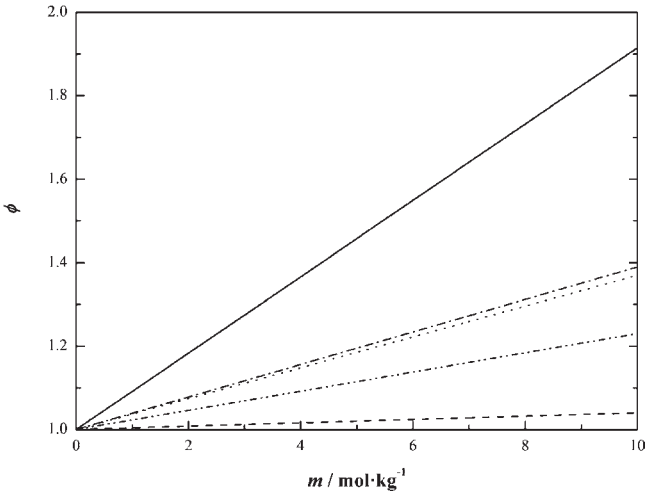

Figure 4. φ of CPA/water binary mixtures with compositions of cryobiological interest; φ, osmotic coefficient; m, molality; —, curve for DMSO/water; — — —, curve for methanol/water; · · ·, curve for EG/water; —·—, curve for PG/water; —· · —, curve for glycerol/water. Curves are calculated with eq 3.

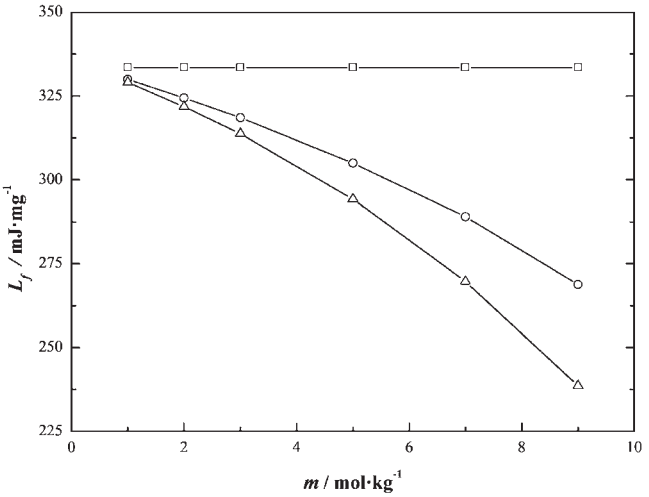

Figure 5. The quantitative relationship between L_f and m considering different effects; L_f, enthalpy of fusion in solutions; m, molality; □, L_0 (L_f without considering the effects of the freezing point depression and the dilution of the solution due to the melting of ice); ○, $L_0 + \Delta H$ (L_f solely considering the effect of the freezing point depression); Δ, L_e (L_f considering both the above-mentioned effects). The lines are just guides to the eye.

composition ranges and the employment of different phase diagrams in the studies.

According to eq 2, the osmolality of the solution increases as the molality rises due to the positive value of B. This trend is clearly presented in Figure 3. By comparatively analyzing the osmotic behaviors of the five CPA solutions, it is found that the aqueous DMSO solution can exert a greater osmotic pressure across cell membranes than other four alcohol solutions corresponding to a certain composition, in particular in the solute-rich region. For example, the 3 mol·kg^{-1} aqueous DMSO solution has an osmolality of 3.83 Osm while EG and glycerol aqueous solutions of the same concentration have osmolalities of 3.33 and 3.25 Osm, respectively. As the solution becomes more concentrated, such differences can be more obvious. The 5 mol·kg^{-1} aqueous DMSO solution has an osmolality of 11.43 Osm while the osmolalities of EG and glycerol aqueous solutions of the same concentration are 2.62 and 3.04 Osm smaller, respectively. Such differences can also be seen in terms of the osmotic virial coefficients. The osmotic virial coefficient for DMSO is always considerably larger than those for other four CPAs as seen in Table 2. A great osmotic pressure across cell membranes can aggravate the efflux of the intracellular water, which is able to reduce the amount of the free water and eventually decrease the amount of the intracellular ice. This phenomenon can in part explain why DMSO is preferably employed in cryopreservation.

Unfrozen Water Content of the Aqueous DMSO Solution. Figure 5 shows the effective enthalpy of fusion L_e in the aqueous DMSO solution of molalities 1−9 mol·kg^{-1}. As seen in Figure 5, the effect of dilution on the latent heat of fusion is non-negligible so that the dilution heat should be taken into consideration for the aqueous DMSO solution to make the calculation results as accurate as possible. The numerical data on the peak area of the melting endotherm of the aqueous DMSO solution are listed in Table 3.

Table 4 illustratively explains the calculation of the unfrozen water content in aqueous DMSO solutions of (1, 3, and 7) mol·kg^{-1}. The complete calculation results of N_{uf}/N_s and W_{uf}/W_t for the aqueous DMSO solutions of (1 to 9) mol·kg^{-1} are shown in Figures 6 and 7.

Table 3. Peak Area A of the Melting Endotherm of the Sample Measured in the Experiment

	1st measurement		2nd measurement		3rd measurement	
m^a	W^b	A	W^b	A	W^b	A
mol·kg^{-1}	mg	mJ	mg	mJ	mg	mJ
1	4.27	1115.48	4.03	1051.57	3.52	917.46
2	3.34	678.13	3.93	785.13	4.13	835.17
3	3.02	459.88	3.93	607.39	4.35	670.06
5	3.42	301.83	4.12	369.39	3.19	290.34
7	4.67	200.91	4.15	195.78	3.64	163.07
9	3.16	53.44	3.65	70.04	3.07	68.22

[a] The molality of the solution. [b] The total mass of the sample.

Figure 6 presents the relationship between N_{uf}/N_s and m for the aqueous DMSO solution. The standard deviations of the results are less than 0.12. It is attention-attracting that the scattered results calculated according to the DSC measurement follow a linear correlation with the molality. Therefore, a linear fit like eq 15 is employed in this study covering a composition range up to 10 mol·kg^{-1}. It should be noticed that this equation will be insufficient for pure water where both the numerator and the denominator of N_{uf}/N_s are zero.

$$\frac{N_{uf}}{N_s} = a_2 + b_2 m \qquad (15)$$

where a_2 and b_2 the fitting parameters, equal to +8.36742 and −0.35438 (mol·kg^{-1})$^{-1}$, respectively. The goodness of fit R^2 of eq 15 is 0.9930.

As seen in Figure 6, a larger molality is always accompanied by a smaller N_{uf}/N_s. The value of N_{uf}/N_s is 8.05 for the dilute solution of 1 mol·kg^{-1} and is 6.43 reducing by 20.1 % for a moderately concentrated solution of 5 mol·kg^{-1}. Further, the

dx.doi.org/10.1021/je2002607 |J. Chem. Eng. Data 2011, 56, 3175–3182

Table 4. Illustrative Examples of Calculation of the Mass Fraction of Unfrozen Water W_{uf}/W_t and the Unfrozen Water Content in mmol per mmol DMSO N_{uf}/N_s in the Aqueous DMSO Solution with eqs 4 to 13

m^a	W^b	$t_m{}^c$	$L_e{}^d$	$W_t{}^e$	$W_s{}^f$	A^g	$W_f{}^h$	$W_{uf}{}^i$		
mol·kg^{-1}	mg	°C	J·g^{-1}	mg	mg	mJ	mg	mg	W_{uf}/W_t	N_{uf}/N_s
1	4.27	−1.62	329	3.96	0.31	1115.48	3.39	0.57	0.143	7.996
3	3.93	−6.35	314	3.18	0.75	607.39	1.93	1.25	0.392	7.267
7	3.64	−19.73	270	2.35	1.29	163.07	0.60	1.75	0.861	5.312

[a] Molality. [b] The total sample mass. [c] The melting temperature. [d] Effective enthalpy of fusion in the solution. [e] The total water mass. [f] The solute mass. [g] Peak area. [h] The freezable water mass. [i] The unfrozen water mass.

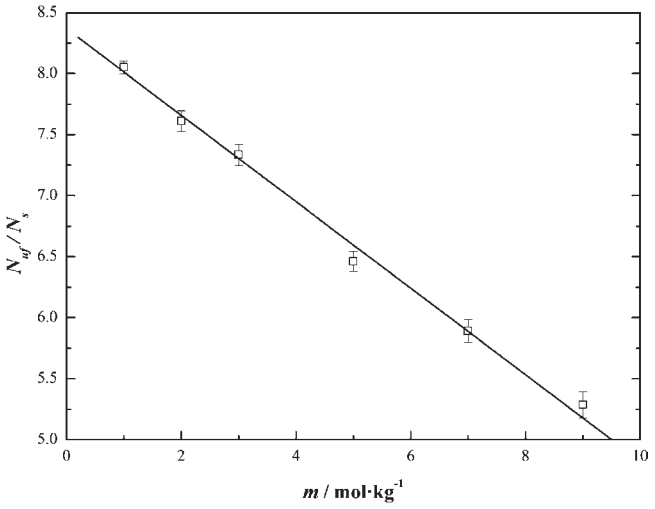

Figure 6. Quantitative relationship between N_{uf}/N_s and m; N_{uf}/N_s, the unfrozen water content in mmol per mmol DMSO; m, molality; —, results calculated with eq 15; □, results calculated based on our experimental data.

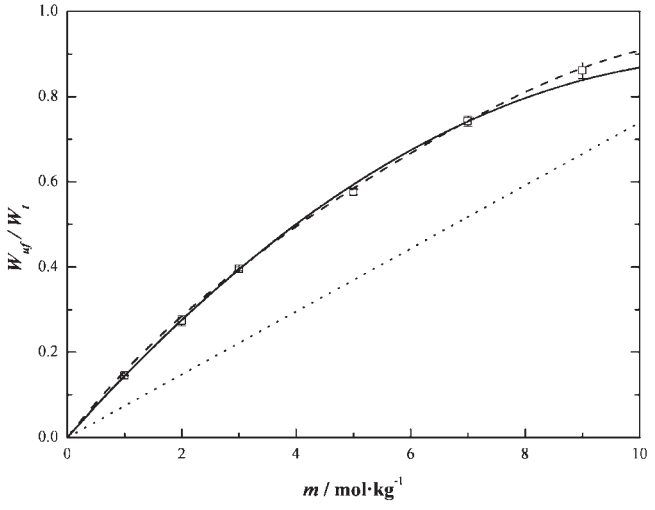

Figure 7. Quantitative relationship between W_{uf}/W_t and m; W_{uf}/W_t, the mass fraction of the unfrozen water; m, molality; —, results calculated with eq 18; – – –, results calculated with eq 19; · · ·, results calculated by the "lever rule" from the liquidus curve; □, results calculated based on our experimental data.

value is 5.28 reducing by 33.4 % for a more concentrated solution of 9 mol·kg^{-1}. The value of N_{uf}/N_s calculated by the "lever rule" is constantly 4.11. The difference between the results in Figure 6 and that given by the "lever rule" reflects the deviation of the nonequilibrium freezing from the equilibrium one. It is clear that such deviation becomes more obvious as the solution is more concentrated.

From the microscopic view, the smaller N_{uf}/N_s indicates the weaker ability of the DMSO molecule to restrict water molecules. This phenomenon can be attributed to the increasing probability of forming DMSO−DMSO hydrogen bonds for one DMSO molecule as more solute molecules exist in the solution. Consequently, the quantity of DMSO−water interactions that one DMSO molecule attends is reduced. These explanations at the molecular level should be proved by molecular dynamics investigations, which is the current work of our research group.

With regard to W_{uf}/W_t, it can be expressed as follows:

$$\frac{W_{uf}}{W_t} = 1000M_w\frac{N_{uf}}{W_t} \quad (16)$$

Considering the molality of the solution $m = N_s/(W_t/1000)$

$$\frac{W_{uf}}{W_t} = M_w m\frac{N_{uf}}{N_s} \quad (17)$$

Therefore, W_{uf}/W_t can be correlated with m according to the following equation:

$$\frac{W_{uf}}{W_t} = a_3 m + b_3 m^2 \quad (18)$$

where the parameters $a_3 = a_2M_w$ and $b_3 = b_2M_w$, equal to 0.15061 $(\text{mol}\cdot\text{kg}^{-1})^{-1}$ and −0.00638 $(\text{mol}\cdot\text{kg}^{-1})^{-2}$, respectively. The goodness of fit R^2 of eq 18 is 0.9659.

The trend $W_{uf}/W_t \sim m$ described by eq 18 is illustrated in Figure 7. The value of W_{uf}/W_t increases as the molality m rises. The value of W_{uf}/W_t rises from 14.4 % to 86.1 % as m increases from (1 to 9) mol·kg^{-1}. The standard deviations of the results are less than 1.9 %.

More water can be blocked by DMSO when the solution departs from the DMSO-deficit region and approaches to the DMSO-rich region, as shown in Figure 7. The previous study concluded that DMSO molecules can perturb the original water−water interactions by strong DMSO-water hydrogen bonds.[4] Hence, it is supposed that more water can be restricted in the intensive DMSO−water interaction network as the unfrozen water when more DMSO molecules present in the solution.

The results of W_{uf}/W_t calculated by the "lever rule" are presented in Figure 7 as well. Since $m(t)$ at −50 °C is constant, W_{uf}/W_t is in direct proportion to m according to the "lever rule". Corresponding to a given molality, the value of W_{uf}/W_t calculated by eq 18 is larger than that given by the "lever rule". In other words, there is more unfrozen water in the residual solution

dx.doi.org/10.1021/je2002607 |J. Chem. Eng. Data 2011, 56, 3175–3182

under nonequilibrium freezing conditions than under equilibrium ones. The finding is consistent with the observation by Boutron,[42] in which the maximum quantity of ice crystallized in aqueous solutions of glycerol was smaller than the quantity of ice in equilibrium with the eutectic.

In addition, a fourth-order fitting representation like eq 19 is also presented by directly fitting our experimental data on W_{uf}/W_t to it. This representation can predict W_{uf}/W_t more precisely as seen in Figure 7 because it avoids the accumulation of errors of N_{uf}/N_s in the above-mentioned theoretical derivation.

$$\frac{W_{uf}}{W_t} = 0.17052m - 0.01697m^2 + 0.00160m^3 - 0.00007m^4 \quad (19)$$

The goodness of fit R^2 of eq 19 is 0.9846.

Ideally, the values of A/W in the three measurements for each m should be equal to one another. This equality can be obeyed by solutions of m up to 7 mol·kg^{-1}, as shown in Table 3. Nonetheless, one can notice a relatively large difference in the measurement for 9 mol·kg^{-1}. In fact, A in the thermogram becomes smaller as the solution is more concentrated. As a result, both the difficulty of accurately determining A and the relative error of the value of A increase. This is one of the reasons why the current study does not focus on solutions of m more than 10 mol·kg^{-1}.

CONCLUSION

This paper presents a DSC experimental study of the osmolality and the unfrozen water content of the aqueous solutions of DMSO. The effect of dilution is taken into account to precisely calculate the unfrozen water content. According to our experimental results, DMSO can depress the freezing point of the aqueous solution more greatly than alcohols like EG and glycerol. It also can exert a great osmotic pressure across cell membranes. Moreover, the amount of the unfrozen water blocked by unit mmol DMSO decreases as the solution becomes more concentrated. On the contrary, the mass fraction of the unfrozen water out of the total water in the aqueous DMSO solution increases as the molality rises. The results in this study can not only enrich the database of physical and chemical properties of dimethyl sulfoxide but deepen our understanding of the cryoprotective mechanisms of dimethyl sulfoxide in aqueous solutions.

AUTHOR INFORMATION

Corresponding Author

*Tel.: +86-411-84708774. Fax: +86-411-84708460. E-mail: wzhongli@dlut.edu.cn.

Funding Sources

The support from the National Nature Science Foundation of China (50976017) and NSFC's Key Program Projects (50736001) is greatly appreciated.

REFERENCES

(1) Naidu, B. V. K.; Rao, K. C.; Subha, M. C. S. Densities and viscosities of mixtures of some glycols and polyglycols in dimethyl sulfoxide at 308.15 K. *J. Chem. Eng. Data* **2002**, *47* (3), 379–382.

(2) Kinart, C. M.; Kinart, W. J.; Skulski, L. Dimethyl sulfoxide–water binary mixtures and their assumed internal structures. *Pol. J. Chem.* **1986**, *60*, 879–900.

(3) Mancera, R. L.; Chalaris, M.; Samios, J. The concentration effect on the 'hydrophobic' and 'hydrophilic' behaviour around DMSO in dilute aqueous DMSO solutions. A computer simulation study. *J. Mol. Liq.* **2004**, *110* (1–3), 147–153.

(4) Yu, Z. W.; Quinn, P. J. Dimethyl sulphoxide: a review of its applications in cell biology. *Biosci. Rep.* **1994**, *14* (6), 259–281.

(5) Betancourt, T.; McMillan, A. F. Vapor-liquid equilibrium of isobutyl alcohol-dimethyl sulfoxide system. *J. Chem. Eng. Data* **1972**, *17* (3), 311–313.

(6) Sassa, Y.; Konishi, R.; Katayama, T. Isothermal vapor-liquid equilibrium data of DMSO [dimethyl sulfoxide] solutions by total pressure method. DMSO-acetone, DMSO-tetrahydrofuran, and DMSO-ethyl acetate systems. *J. Chem. Eng. Data* **1974**, *19* (1), 44–48.

(7) Srivastava, A. K.; Shankar, S. L. Ionic Conductivity in Binary Solvent Mixtures. 3. Dimethyl Sulfoxide+ Propylene Carbonate at 25 °C. *J. Chem. Eng. Data* **1998**, *43* (1), 25–28.

(8) Srivastava, A. K.; Shankar, S. L. Ionic Conductivity in Binary Solvent Mixtures. 4. Dimethyl Sulfoxide + Water at 25 °C. *J. Chem. Eng. Data* **1999**, *45* (1), 92–96.

(9) Trehan, A.; Kohn, J. P.; Bibbs, D. G. Phase equilibrium behavior of the ethane+ dimethyl sulfoxide and ethane+ quinoline binary systems. *J. Chem. Eng. Data* **1994**, *39* (4), 842–847.

(10) Lovelock, J. E.; Bishop, M. W. H. Prevention of freezing damage to living cells by dimethyl sulphoxide. *Nature* **1959**, *183*, 1394–1395.

(11) Rasmussen, D. H.; MacKenzie, A. P. Phase diagram for the system water–dimethylsulphoxide. *Nature* **1968**, *220*, 1315–1317.

(12) Pegg, D. E. Equations for obtaining melting points and eutectic temperatures for the ternary system dimethyl sulphoxide/sodium chloride/water. *Cryo Lett.* **1986**, *7*, 387–394.

(13) Fahy, G. M. Analysis of "solution effects" injury. Equations for calculating phase diagram information for the ternary systems NaCl-dimethylsulfoxide-water and NaCl-glycerol-water. *Biophys. J.* **1980**, *32* (2), 837–850.

(14) Hey, J. M.; MacFarlane, D. R. Crystallization of ice in aqueous solutions of glycerol and dimethyl sulfoxide. 1. A comparison of mechanisms. *Cryobiology* **1996**, *33* (2), 205–216.

(15) Hey, J. M.; MacFarlane, D. R. Crystallization of Ice in Aqueous Solutions of Glycerol and Dimethyl Sulfoxide 2: Ice Crystal Growth Kinetics. *Cryobiology* **1998**, *37* (2), 119–130.

(16) Baudot, A.; Alger, L.; Boutron, P. Glass-Forming Tendency in the System Water-Dimethyl Sulfoxide. *Cryobiology* **2000**, *40* (2), 151–158.

(17) Fuller, B. J. Cryoprotectants: the essential antifreezes to protect life in the frozen state. *Cryo Lett.* **2004**, *25* (6), 375–388.

(18) Jain, J. K.; Paulson, R. J. Oocyte cryopreservation. *Fertil. Steril.* **2006**, *86* (4), 1037–1046.

(19) Elliott, J. A. W.; Prickett, R. C.; Elmoazzen, H. Y.; Porter, K. R.; McGann, L. E. A multisolute osmotic virial equation for solutions of interest in biology. *J. Phys. Chem. B* **2007**, *111* (7), 1775–1785.

(20) Prickett, R. C.; Elliott, J. A. W.; Hakda, S.; McGann, L. E. A non-ideal replacement for the Boyle van't Hoff equation. *Cryobiology* **2008**, *57* (2), 130–136.

(21) Elmoazzen, H. Y.; Elliott, J. A. W.; McGann, L. E. Osmotic transport across cell membranes in nondilute solutions: a new nondilute solute transport equation. *Biophys. J.* **2009**, *96* (7), 2559–2571.

(22) Prickett, R. C.; Elliott, J. A. W.; McGann, L. E. Application of the osmotic virial equation in cryobiology. *Cryobiology* **2010**, *60* (1), 30–42.

(23) Lee, K. Y.; Ha, W. S. DSC studies on bound water in silk fibroin/S-carboxymethyl kerateine blend films. *Polymer* **1999**, *40* (14), 4131–4134.

(24) Liu, W. G.; Yao, K. D. What causes the unfrozen water in polymers: hydrogen bonds between water and polymer chains? *Polymer* **2001**, *42* (8), 3943–3947.

(25) Yudianti, R.; Karina, M.; Sakamoto, M.; Azuma, J. DSC Analysis on Water State of Salvia Hydrogels. *Macromol. Res.* **2009**, *17* (12), 1015–1020.

(26) Hager, S. L.; Macrury, T. B. Investigation of phase behavior and water binding in poly (alkylene oxide) solutions. *J. Appl. Polym. Sci.* **1980**, *25* (8), 1559–1571.

(27) Weng, L.; Li, W.; Zuo, J. DSC determination of partial ternary phase diagrams of methanol/sodium chloride/water and propylene glycol/sodium chloride/water and their applications for synthesized diagrams. *Thermochim. Acta* **2011**, *512* (1−2), 225–232.
(28) Goodman, S. R. *Medical Cell Biology*; Lippincott-Raven: New York, 1998.
(29) Weng, L.; Li, W.; Zuo, J. Kinetics of osmotic water flow across cell membranes in non-ideal solutions during freezing and thawing. *Cryobiology* **2010**, *61* (2), 194–203.
(30) Asaoka, T.; Kumano, H.; Okada, M.; Kose, H. Effect of temperature on the effective latent heat of fusion of ice in aqueous solutions. *Int. J. Refrig.* **2010**, *33* (8), 1533–1539.
(31) Kumano, H.; Asaoka, T.; Saito, A.; Okawa, S. Formulation of the latent heat of fusion of ice in aqueous solution. *Int. J. Refrig.* **2009**, *32* (1), 175–182.
(32) Angell, C. A.; Sichina, W. J.; Oguni, M. Heat capacity of water at extremes of supercooling and superheating. *J. Phys. Chem.* **1982**, *86* (6), 998–1002.
(33) Giauque, W. F.; Stout, J. W. The Entropy of Water and the Third Law of Thermodynamics. The Heat Capacity of Ice from 15 to 273 K. *J. Am. Chem. Soc.* **1936**, *58* (7), 1144–1150.
(34) Redlich, O.; Kister, A. T. Algebraic representation of thermodynamic properties and the classification of solutions. *Ind. Eng. Chem.* **1948**, *40* (2), 345–348.
(35) Barrio, M.; Tamarit, J. L.; Céolin, R.; Pardo, L. C.; Negrier, P.; Mondieig, D. Connecting the normal pressure equilibria of the two-component system CCl (CH3) 3+ CBrCl3 to the pressure-temperature phase diagrams of pure components. *Chem. Phys.* **2009**, *358* (1−2), 156–160.
(36) Kracht, C.; Ulbig, P.; Schulz, S. Measurement and correlation of excess molar enthalpies for (ethanediol, or 1, 2-propanediol, or 1, 2-butanediol+ water) at the temperatures (285.65, 298.15, 308.15, 323.15, and 338.15) K. *J. Chem. Thermodyn.* **1999**, *31* (9), 1113–1127.
(37) Kaptay, G. A new equation for the temperature dependence of the excess Gibbs energy of solution phases. *Calphad* **2004**, *28* (2), 115–124.
(38) Clever, H. L.; Pigott, S. P. Enthalpies of mixing of dimethylsulfoxide with water and with several ketones at 298.15 K. *J. Chem. Thermodyn.* **1971**, *3* (2), 221–225.
(39) Han, X.; Liu, Y.; Critser, J. K. Determination of the quaternary phase diagram of the water-ethylene glycol-sucrose-NaCl system and a comparison between two theoretical methods for synthetic phase diagrams. *Cryobiology* **2010**, *61* (1), 52–57.
(40) Woods, E. J.; Bagchi, A.; Benson, J. D.; Han, X.; Critser, J. K. Melting point equations for the ternary system water/sodium chloride/ethylene glycol revisited. *Cryobiology* **2008**, *57* (3), 336.
(41) Kleinhans, F. W.; Mazur, P. Comparison of actual vs. synthesized ternary phase diagrams for solutes of cryobiological interest. *Cryobiology* **2007**, *54* (2), 212–222.
(42) Boutron, P. More accurate determination of the quantity of ice crystallized at low cooling rates in the glycerol and 1, 2-propanediol aqueous solutions: Comparison with equilibrium. *Cryobiology* **1984**, *21* (2), 183–191.